Archives of Biochemistry and Biophysics 606 (2016) 10–15

Contents lists available at ScienceDirect

Archives of Biochemistry and Biophysics

journal homepage: www.elsevier.com/locate/yabbi

Protein complex formation and intranuclear dynamics of NAC1 in cancer cells

Naomi Nakayama [a], Hiroaki Kato [a], Gyosuke Sakashita [a], Yuko Nariai [a], Kentaro Nakayama [b], Satoru Kyo [b], Takeshi Urano [a, *]

[a] Department of Biochemistry, Shimane University School of Medicine, Izumo 693-8501, Japan
[b] Department of Obstetrics and Gynecology, Shimane University School of Medicine, Izumo 693-8501, Japan

ARTICLE INFO

Article history:
Received 2 June 2016
Received in revised form
1 July 2016
Accepted 11 July 2016
Available online 14 July 2016

Keywords:
Nucleus accumbens-associated protein 1 (NAC1)
Protein complex formation
Intranuclear dynamics
Live cell photobleaching analysis
Fluorescence recovery after photobleaching (FRAP)
Fluorescence loss in photobleaching (FLIP)

ABSTRACT

Nucleus accumbens-associated protein 1 (NAC1) is a cancer-related transcription regulator protein that is also involved in the pluripotency and differentiation of embryonic stem cells. NAC1 is overexpressed in various carcinomas including ovarian, cervical, breast, and pancreatic carcinomas. NAC1 knock-down was previously shown to result in the apoptosis of ovarian cancer cell lines and to rescue their sensitivity to chemotherapy, suggesting that NAC1 may be a potential therapeutic target, but protein complex formation and the dynamics of intranuclear NAC1 in cancer cells remain poorly understood. In this study, analysis of HeLa cell lysates by fast protein liquid chromatography (FPLC) on a sizing column showed that the NAC1 peak corresponded to an apparent molecular mass of 300–500 kDa, which is larger than the estimated molecular mass (58 kDa) of the protein. Furthermore, live cell photobleaching analyses with green fluorescent protein (GFP)-fused NAC1 proteins revealed the intranuclear dynamics of NAC1. Collectively our results demonstrate that NAC1 forms a protein complex to function as a transcriptional regulator in cancer cells.

1. Introduction

Nucleus accumbens-associated protein 1 (NAC1), encoded by the *NACC1* gene, is a nuclear protein that harbors an *N*-terminal BTB/POZ (**b**road complex, **t**ramtrack, **b**ric-a-brac/**po**xvirus and **z**inc finger) (hereafter abbreviated BTB) and a *C*-terminal BEN (**B**ANP, **E**5R and **N**AC1) domain (Fig. 1A). The BTB domain is a ~100 amino acid highly conserved motif that mediates homodimerization and/or heterodimerization and interacts with other proteins [1,2]. NAC1 homodimerizes through its BTB domain [3] and heterodimerizes with Myc-interacting zinc-finger protein 1 (Miz1) through the respective BTB domain [4,5]. Most BTB proteins contain other *C*-terminal functional domains, such as DNA-binding zinc fingers. NAC1 lacks these characteristic DNA-binding domains but instead contains a *C*-terminal BEN domain, identified through computational analysis in 2008, which may mediate protein-DNA and protein-protein interactions [6].

NAC1 participates in various biological processes. NAC1 was originally identified and cloned as a cocaine-inducible transcript from the nucleus accumbens, a unique forebrain structure involved in reward motivation and addictive behavior [7]. NAC1 is known to be important for the pluripotency of embryonic stem cells [8,9]. Recently, NAC1 was shown to promote mesendodermal and repress neuroectodermal fate selection in embryonic stem cells, in cooperation with other pluripotency transcription factors, Oct4, Sox2, and Tcf3 [10]. *NACC1* knockout mouse embryos and newborns exhibit a lower survival rate for embryos or newborns, with surviving mice showing defective bony patterning in the vertebral axis [11].

NACC1 was also identified as a cancer-associated BTB gene by serial analysis of gene expression in ovarian cancer cells [12]. NAC1 is significantly overexpressed in several types of carcinomas including ovarian, colorectal, breast, renal cell, cervical, and pancreatic carcinomas is associated with tumor growth and survival, and increases the resistance of tumor cells to chemotherapy [12–22]. These reports suggested that NAC1 plays a driver role in cancer development and that it might be a potential therapeutic target.

Although NAC1 appears to play increasingly significant and

* Corresponding author.
E-mail address: turano@med.shimane-u.ac.jp (T. Urano).

http://dx.doi.org/10.1016/j.abb.2016.07.007
0003-9861/

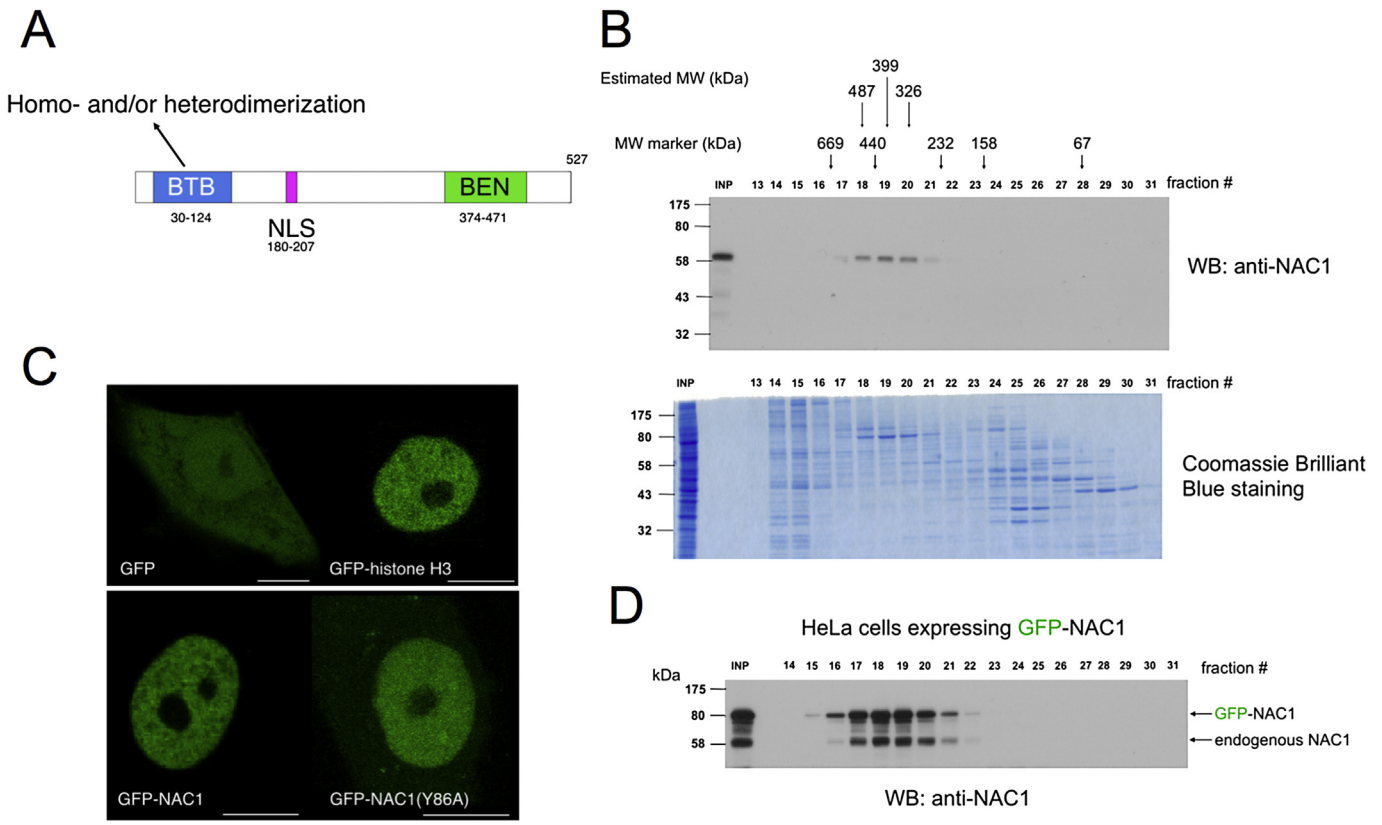

Fig. 1. NAC1 protein complex in cancer cells. (A) Schematic representation of human NAC1 protein showing the BTB domain, nuclear localization signal (NLS), and the BEN domain. (B) Protein extracts of HeLa cells were analyzed by size exclusion chromatography on a FPLC Superdex 200 column. Protein mass standards are indicated above the graph: thyroglobulin (669 kDa), ferritin (440 kDa), catalase (232 kDa), aldolase (158 kDa) and bovine serum albumin (67 kDa). The estimated molecular weights of fractions 18 to 20 were calculated using the standard curve. The eluted fractions were analyzed by Coomassie staining and Western blot using anti-NAC1 antibody 9.27. (C) A representative HeLa cell stably expressing GFP, GFP-histone H3, GFP-NAC1, or GFP-NAC1(Y86A). Images were obtained under a 473 diode laser. Bars, 10 μm. (D) Protein extracts of HeLa cells stably expressing GFP-NAC1 were analyzed by size exclusion chromatography on a FPLC Superdex 200 column. Eluted fractions were analyzed by Western blot using anti-NAC1 antibody 9.27.

diverse functions in cancer and stem cell biology, protein complex formation and the dynamics of intranuclear NAC1 in cells are poorly understood. In this study, we fractionated NAC1-containing complexes according to mass by gel size-exclusion column chromatography and investigated the intranuclear dynamics of NAC1 by live cell photobleaching analysis.

2. Materials and methods

2.1. Plasmid construction

Human histone H3 full-length cDNA obtained by reverse transcribed PCR using the total RNA from HeLa cells was cloned into pMXs-FHG. All PCR-amplified cDNA products were fully sequenced using a 3130 genetic analyzer (ThermoFisher Scientific, Waltham, MA, USA) to confirm the sequences and to verify the absence of secondary point mutations.

2.2. Cell culture

The HeLa human cervical epithelioid carcinoma cell line was purchased from the Japanese Collection of Research Bioresources (JCRB) Cell Bank (JCRB9004). To maintain authenticity of the cell line, multiple aliquots of frozen stocks were prepared from initial stocks, and every 3 months, a new frozen stock was used for the experiments. The cells were routinely inspected for identity by morphology and growth curve analysis and validated to be *mycoplasma* free. HeLa cells expressing GFP, GFP-NAC1, or GFP-NAC1(Y86A) have been described [23]. The GFP is Emerald GFP (ThermoFisher Scientific) (made monomeric by introducing the mutation A206K) (hereafter abbreviated GFP). HeLa cells expressing GFP-histone H3 were established by utilizing a retrovirus infection system [23]. Overexpression of NAC1 proteins gives rise to the formation of dense body-like structures in the nucleus [12,24]. Only GFP-positive cells expressing the lowest detectable amounts of fusion protein were isolated using a FACSAris II cell sorter and FACSDiva software (BD, Franklin Lakes, NJ, USA). All cells were grown in Dulbecco's modified Eagle's medium (Nissui, Tokyo, Japan) supplemented with 10% (v/v) fetal bovine serum (Sigma-Aldrich, St. Louis, MO, USA).

2.3. Molecular mass determination

The molecular mass of endogenous NAC1 in HeLa cells was estimated by fast protein liquid chromatography (FPLC) gel filtration on a Superdex 200 Increase 10/300 GL column (GE Healthcare, Buckinghamshire, UK) by comparison with protein molecular weight markers. The markers were thyroglobulin (669 kDa), ferritin (440 kDa), catalase (232 kDa), aldolase (158 kDa) and bovine serum albumin (67 kDa). One % (v/v) Triton X-100 lysate of HeLa cells and markers were separately loaded on the column and eluted with 0.50 mM phosphate buffer (pH 7.0) containing 0.15 M NaCl. Fractions (0.5 ml) were collected and proteins were resolved by SDS-PAGE. NAC1 was detected on immunoblots with anti-NAC1 monoclonal antibody 9.27 [23]. The exponential equation of the standard curve was $y = 17816e^{-0.2x}$ ($R^2 = 0.9991$) (y = estimated

molecular mass, x = fraction number).

2.4. FRAP and FLIP analyses

Fluorescent images were acquired using an FV1000 laser scanning confocal unit coupled to an inverted microscope (model IX81; Olympus, Tokyo, Japan) equipped with a ×100 oil immersion objective (UPLSAPO 100XO, NA 1.40, Olympus) and analyzed using Fluoview software (Olympus). Cells were maintained at 37 °C in a Tokai Hit incubation system for microscopes (Tokai Hit, Shizuoka, Japan). Cells were analyzed on 35 mm glass-bottom dishes (IWAKI, Tokyo, Japan) in CO_2-independent medium (ThermoFisher Scientific, Waltham, MA, USA) to avoid medium acidification in the CO_2-free atmosphere. A 473 nm laser (laser power: 0.1%) was used to excite GFP. A square region of interest (ROI) of 150 × 150 pixels (1 pixel = 0.124 μm) was scanned with a 2-line Kalman filter to obtain a noise-free image ideal for intensity measurements.

For FRAP experiments, five and 95 images (scanning time: 456 ms/frame) were acquired before and after bleaching, respectively. Photobleaching was performed by creating a bleach spot of 8 × 8 pixels using the Tornado mode of the FV1000 confocal unit (bleaching time: 250 ms; laser power: 100%). Using this bleaching condition, the bleaching constant (K) and the half width of the beam (w) were estimated to be 3.56 ± 0.432 and 1.63 ± 0.145, respectively. The intensities in the bleached area (B), unbleached area (U), and the background (bg) in each post-bleach image were measured to obtain the intensity ratio (R_n): $R_n = (B-bg)/(U-bg)$. R_n values were divided by the average intensity ratio (R_0) of the five pre-bleach images to obtain normalized FRAP values (R): $R = R_n/R_0$. We defined the time point when R reached 0.5 as $t_{1/2}$. For each condition, the mean and SD of at least 35 individual FRAP values were calculated to draw the plots. The normalized FRAP values were used to calculate the diffusion coefficient (D) by curve fitting with the method of least squares [25,26]. D for GFP-NAC1-WT and GFP-NAC1(Y86A) in the nucleus were 0.174 and 0.569 $\mu m^2/s$, respectively. Welch's two sample t-test was used in the FRAP analysis to calculate p values; ***, $p < 0.001$.

FLIP experiments were conducted using the time controller function of the FV1000, according to the manufacturer's instructions. Five pre-bleach images were acquired before beginning 50 bleach-scan cycles. In a bleach-scan cycle, half of the ROI (150 × 75 pixels) was bleached once (laser power: 100%) before scanning a post-bleach image (150 × 150 pixels). Intensity ratios of the pre- and post-bleach images were calculated to obtain normalized FLIP values, as in the FRAP experiments. For each condition, the mean and SD values for at least 8 individual FLIP values were calculated to draw the plots.

3. Results

3.1. NAC1 forms a 300–500 kDa protein complex or complexes in cancer cells

We have recently shown that NAC1 harbors an unusual bipartite-type nuclear localization signal (NLS) to exert transcriptional regulator functions (Fig. 1A) [23]. Complex formation and the dynamics of intranuclear NAC1 in cancer cells remain poorly understood. To investigate whether NAC1 forms a protein complex or complexes in cancer cells, we fractionated of 1% (v/v) Triton X-100 HeLa cell lysates according to mass using fast protein liquid chromatography (FPLC) on a Superdex 200 sizing column. The estimated molecular mass of human NAC1 protein is 58 kDa. Coomassie staining of proteins from whole cell lysates showed no visible protein bands corresponding to NAC1 (Fig. 1B, *lower panel*). However, immunoblot analysis clearly showed endogenous NAC1 in HeLa cells in a major peak (Fig. 1B, *upper panel*). The peak (fractions 18 to 20) corresponded to a calculated molecular mass of 300–500 kDa. NAC1 homodimerizes, and heterodimerizes with Myc-interacting zinc-finger protein 1 (Miz1, 88 kDa), through the BTB domains [3,4,23]. These results suggested that human NAC1 forms a protein complex in cancer cells and that other BTB-containing transcriptional regulator may be a partner of NAC1.

3.2. Intranuclear dynamics of NAC1 in living cells

To study the dynamics of NAC1 protein within live human cancer cells, NAC1 was fused to green fluorescent protein (GFP) at the N terminal (GFP-NAC1). Overexpression of NAC1 results in the formation of dense body-like structures in the nucleus [12,24]. Only GFP-positive cells expressing the lowest detectable amounts of fusion protein were isolated using a FACSAris II cell sorter after retrovirus transfection. Live-cell imaging during the cell cycle conducted to monitor the subcellular distribution of GFP-NAC1 in HeLa cells demonstrated that GFP-NAC1 localized to the nucleus and was excluded from the nucleoli, similar to endogenous NAC1 [23]. HeLa cell lines stably expressing GFP, GFP-NAC1, GFP-NAC1(Y86A) or GFP-histone H3 were generated (Fig. 1C). NAC1(Y86A), in which a conserved tyrosine residue within the BTB domain of NAC1 was replaced with alanine was previously shown not to dimerize [23], as predicted by earlier structural information [3].

We then assessed the ability of GFP-NAC1 to form protein complexes in HeLa cells. Triton-X 100 (1% v/v) lysate of HeLa cells expressing GFP-NAC1 was fractionated using the Superdex 200 sizing column and provided peaks similar to the peaks obtained using lysates of cell expressing endogenous NAC1 (Fig. 1D). This indicated that GFP-NAC1 forms a 300–500 kDa protein complex or complexes in cancer cells and demonstrated that complex formation is not affected by the GFP tag. It is noteworthy that the protein levels of GFP-NAC1 and endogenous NAC1 were comparable. Taken together, these results show that GFP-NAC1 behaves similarly to endogenous NAC1 in cells, allowing the use of GFP-NAC1 to investigate the spatiotemporal regulation of the endogenous protein in live human cancer cells.

The behavior of NAC1 protein in live human cells was investigated using real-time *in vivo* confocal fluorescence microscopy. Asynchronized HeLa cells stably expressing GFP-NAC1, or GFP-NAC1(Y86A) were subjected to fluorescence recovery after photobleaching (FRAP), a technique commonly used to study the diffusional behavior of nuclear proteins [27–29]. In parallel, HeLa cells stably expressing a freely diffusing GFP, or a very stable chromatin binding histone H3 fused with GFP (GFP-histone H3), were analyzed for comparison. The mobility and kinetic properties of GFP, NAC1, NAC1(Y86A) and histone H3 were assessed by photobleaching the GFP-tagged proteins in a small circular region (8 pixels in diameter; 1 pixel = 0.124 μm) located inside the nucleus and then monitoring the recovery of fluorescence over time (Fig. 2A). Fig. 2B and supplementary movies (videos S1, S2, and S3) show the results of typical FRAP experiments. Mean normalized curves derived from at least 35 individual cells are shown in Fig. 2C. Although no immobile fraction was observed, NAC1 showed significantly slower recovery kinetics ($t_{½}$ = 3.19 ± 1.21 s) than that of freely diffusing GFP ($t_{½}$ = 0.66 ± 0.25 s) (Fig. 2D). We also measured the diffusion coefficient (D) values by fitting the normalized curves to the standard equation [27], representing the rate at which a protein repopulates a photobleached area (Fig. 2B). These measurements confirmed that NAC1 had lower mobility in the live cancer cell nucleus (D = 0.174 $\mu m^2/s$) compared to the GFP control. Importantly, the D value for NAC1 in the nucleus is comparable to those previously reported for nucleosomal binding

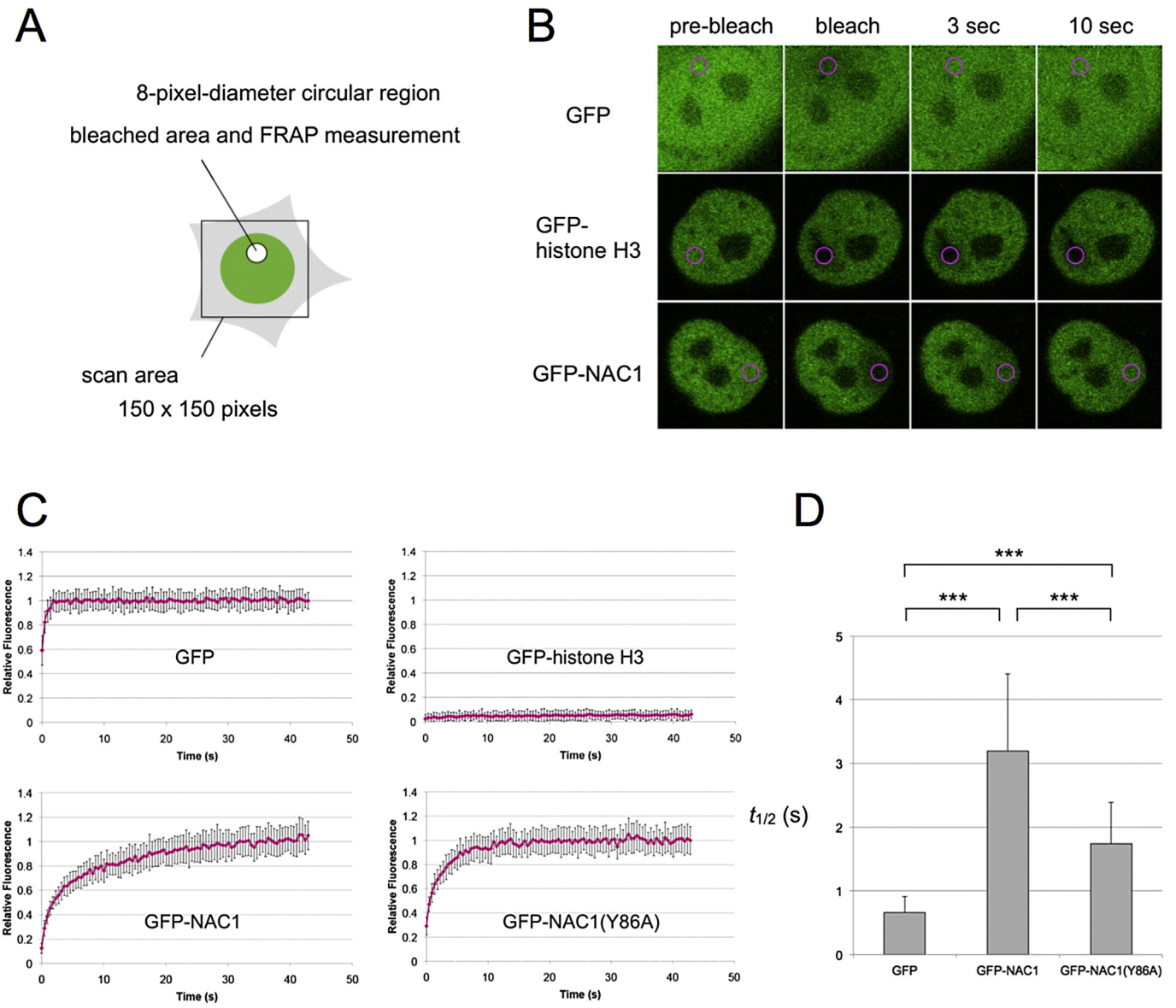

Fig. 2. Fluorescence recovery after photobleaching (FRAP) for the analysis of NAC1 dynamics in HeLa cells. (A) Schematic drawing of FRAP analysis. (B) Representative images of FRAP analysis in living HeLa cells stably expressing GFP, GFP-histone H3 or GFP-NAC1. The bleach areas are marked with magenta circles. The fluorescence recovery was monitored and is shown at the indicated time points after bleaching. See supplementary videos S1 (GFP), S2 (GFP-histone H3) and S3 (GFP-NAC1). Quantitative FRAP analysis (FRAP recovery curves) (C) and $t_{1/2}$ analysis (D) of stably expressed GFP, GFP-histone H3, GFP-NAC1 or GFP-NAC1(Y86A) in HeLa cells. Each value is the mean ± SD. ***, $p < 0.001$; calculated with Welch's two sample *t*-test.

proteins such as HMG-17 [30]. Moreover, this value is much lower than values reported for freely diffusing GFP in the nucleus [31]. Taken together, these findings suggest that a substantial fraction of NAC1 in the nucleus is associated with or interacts with nuclear proteins or chromatin, thereby significantly decreasing their mobility.

Supplementary video related to this article can be found at http://dx.doi.org/10.1016/j.abb.2016.07.007.

The BTB domain of NAC1 mediates homodimerization or heterodimerization with Miz1 [3,4]. We therefore addressed how dimer formation by NAC1 contributes to its dynamics within the cancer cell nucleus. We utilized the Y86A point mutant of NAC1, which does not form dimers [23]. NAC1(Y86A) displayed significantly faster recovery kinetics ($t_{½}$ = 1.74 ± 0.65 s) compared to NAC1 ($t_{½}$ = 3.19 ± 1.21 s) (Fig. 2D), but was significantly slower than that of freely diffusing GFP ($t_{½}$ = 0.66 ± 0.25 s). The *D* value (0.569 $\mu m^2/s$) of NAC1(Y86A) was around 3 to 4 times higher than that of NAC1(0.174 $\mu m^2/s$). Thus, dimer formation by NAC1 coincided with significantly slower diffusion in the nucleus.

We next employed a complementary approach, fluorescence loss in photobleaching (FLIP), in which a high-power laser beam bleaches the same area in a cell repeatedly and the signal intensity is measured at the bleached and unbleached areas in the fluorescing cell (Fig. 3A). FLIP experiments therefore measure signal decay rather than fluorescence recovery and are useful to determine protein mobility, as well as protein shuttling between cellular compartments [32,33]. Fig. 3B and supplementary movies (videos S4, S5, and S6) show typical results from the FLIP experiments. Repetitive bleaching of the GFP-NAC1 signal in one half of the nucleus led to gradual fluorescence loss in the other half of the nucleus, and resulted in a complete loss of fluorescence from the entire nucleus within 3 min (Fig. 3B and C, GFP-NAC1, compare GFP

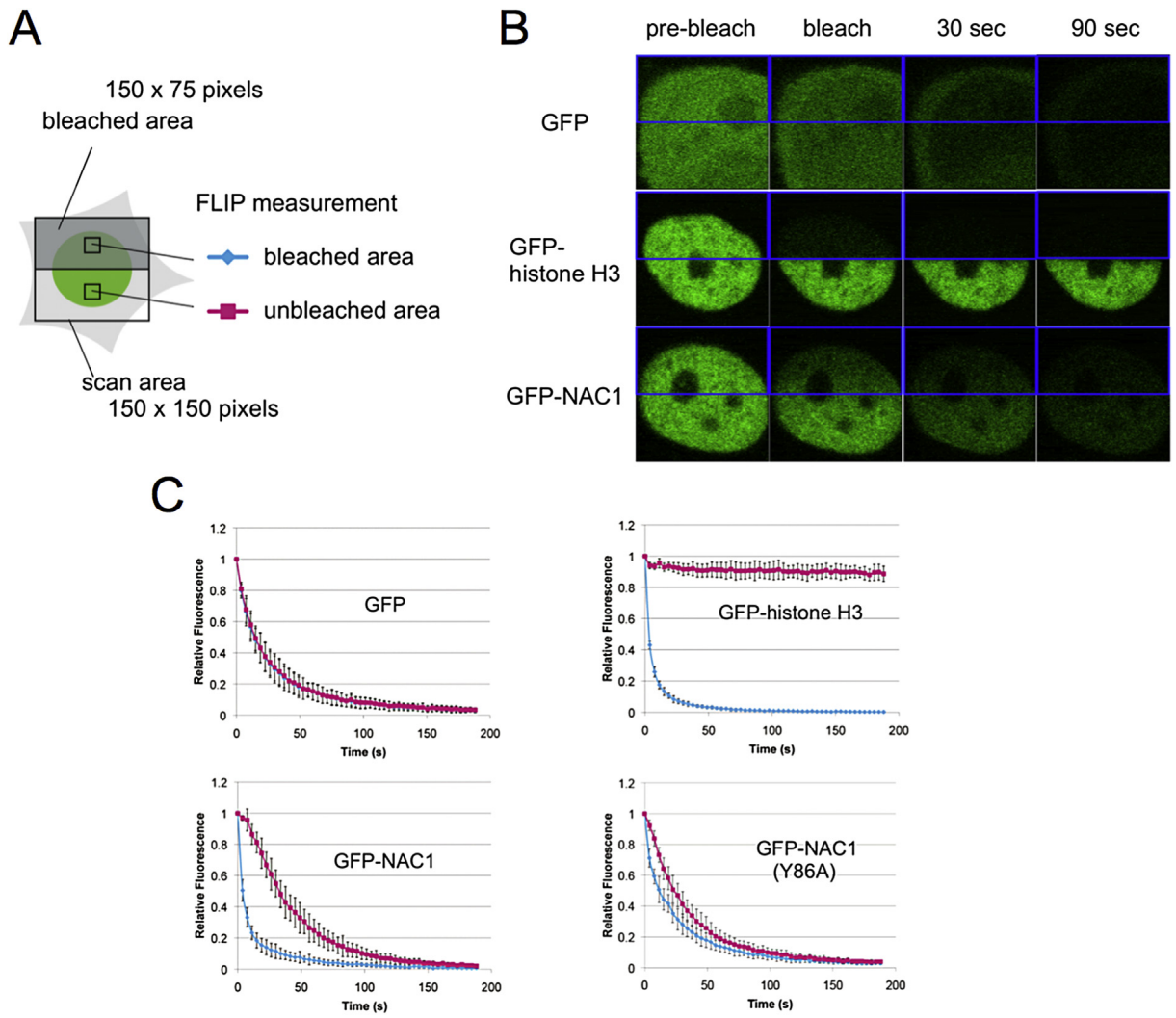

Fig. 3. Fluorescence loss in photobleaching (FLIP) for the analysis of NAC1 dynamics in HeLa cells. (A) Schematic drawing of FLIP analysis. (B) Representative sequence of images from FLIP time course experiments in living HeLa cells stably expressing GFP, GFP-histone H3 or GFP-NAC1. The bleached areas are marked with blue squares. See supplementary videos S4 (GFP), S5 (GFP-histone H3) and S6 (GFP-NAC1). (C) Quantitative FLIP analysis of stably expressed GFP, GFP-histone H3, GFP-NAC1 and GFP-NAC1(Y86A) in HeLa cells. The fluorescence loss was monitored in the bleached (blue) and control unbleached (magenta) regions. Each value is the mean ± SD.

and GFP-histone H3). Consistent with the FRAP data, this result indicates that NAC1 in the nucleus is highly mobile and rapidly exchanges with unbleached GFP-NAC1 molecules in the nucleus, although its diffusion is slower than that of freely diffusing GFP. Furthermore, the GFP-NAC1(Y86A) mutant showed a considerably faster loss of fluorescence in the unbleached half of the nucleus compared with that of wild-type GFP-NAC1 (Fig. 3C). Therefore, the intranuclear mobility of NAC1 correlated with dimer formation and is probably dependent on the binding of NAC1 to other nuclear proteins or chromatin.

Supplementary video related to this article can be found at http://dx.doi.org/10.1016/j.abb.2016.07.007.

4. Discussion

The present study indicates that NAC1 forms 300–500 kDa protein complexes in HeLa cervical cancer cells. We previously reported that high NAC1 expression in either solid tumors or effusions was significantly correlated with shorter progression-free survival in ovarian cancer patients [12,34]. In pancreatic adenocarcinoma, conversely, a low NAC1 expression level was related to worse oncologic features such as incidence of lymphatic metastasis, venous invasion, and high TNM grading [22]. In neuronal cells, NAC1 is known to interact with the histone deacetylases HDAC3 (49 kDa) and HDAC4 (119 kDa) [35], and with REST corepressor 1 (CoREST, 53 kDa) [36], but not with other corepressors (Nuclear receptor corepressor 1 (NCoR), Nuclear receptor corepressor 2 (NCoR2, also known as SMRT), or mSin3a) [35]. It is conceivable that NAC1 forms a relatively large molecular complex that functions as a repressor complex in neuronal cells. Unfortunately, the molecular mass of this complex has not been elucidated. Given that the ovary, pancreas and neurons originate from the mesoderm, endoderm and ectoderm, respectively, NAC1 may have diverse functions in different cancer cell types, and between cancer and neuronal cells. It is therefore important to specifically identify the additional components of the NAC1-containing complex or complexes in cancer and neuronal cells.

We imaged the dynamics of NAC1 and measured its kinetics in cancer nuclei using photobleaching techniques (FRAP and FLIP). The novelty of our study lies in it providing the first description of NAC1 dynamics. After collecting photobleaching data during FRAP analysis, we determined two general parameters; the $t_{1/2}$ of the

fluorescence recovery, and the diffusion coefficient (D). Determining a D value is useful because it can be compared across a wide range of reported results, whereas $t_{1/2}$ values can only be directly compared for experiments conducted using an identical microscope setup and imaging parameters [32]. Parameters that directly influence D include the viscosity (or crowdedness) of the environment, protein interactions with large or immobilized molecules, or combinations of these variables [32]. The D values for NAC1 (0.174 $\mu m^2/s$) and NAC1(Y86A; incapable of dimerization) (0.569 $\mu m^2/s$) measured in the current study are much lower than the value reported for freely diffusing GFP (50 $\mu m^2/s$) in the nucleus [31]. This indicates that a substantial fraction of NAC1 in the nucleus is associated with or interacts with nuclear proteins or chromatin, depending on whether NAC1 forms a dimer. These $t_{1/2}$ values obtained under the same conditions by FRAP analysis (Fig. 2D) and FLIP analysis (Fig. 3B and C) support this conclusion.

In this study, we showed that NAC1 forms 300–500 kDa complexes in cancer cells. Additionally, we demonstrated that a substantial fraction of NAC1 in the nucleus is associated with or interacts with nuclear proteins or chromatin, depending on whether NAC1 forms a dimer. Homo- or heterodimerization is frequently observed in transcription factors [37]. Like other transcription factors the dimerization of NAC1 might raise the affinity and specificity of DNA recognition, as well as provide diversity in the formation of regulatory complexes, which contribute to the intranuclear dynamics of NAC1. Efforts to identify the other components of the NAC1-containing complex or complexes in different types of cancer cells and embryonic stem cells will provide important insights into how NAC1 regulates the transcription of genes involved in oncogenicity and pluripotency.

Acknowledgement

We acknowledge the technical expertise of the Center for Integrated Research in Science at Shimane University. We also thank Yuko Fukuma for technical assistance. This work was supported by the SUIGAN Project, Shimane University. The authors have no conflicts to interest to declare.

References

[1] T. Collins, J.R. Stone, A.J. Williams, All in the family: the BTB/POZ, KRAB, and SCAN domains, Mol. Cell. Biol. 21 (2001) 3609–3615.
[2] P.J. Stogios, G.S. Downs, J.J. Jauhal, S.K. Nandra, G.G. Privé, Sequence and structural analysis of BTB domain proteins, Genome Biol. 6 (2005) R82.
[3] M.A. Stead, S.B. Carr, S.C. Wright, Structure of the human Nac1 POZ domain, Acta Crystallogr. Sect. F Struct Biol.Cryst. Commun. 65 (2009) 445–449.
[4] M.A. Stead, S.C. Wright, Nac1 interacts with the POZ-domain transcription factor, Miz1, Biosci. Rep. 34 (2014) e00110.
[5] M.A. Stead, S.C. Wright, Structures of heterodimeric POZ domains of Miz1/BCL6 and Miz1/NAC1, Acta Crystallogr. F. Struct. Biol. Commun. 70 (2014) 1591–1596.
[6] S. Abhiman, L.M. Iyer, L. Aravind, BEN: a novel domain in chromatin factors and DNA viral proteins, Bioinformatics 24 (2008) 458–461.
[7] X.Y. Cha, R.C. Pierce, P.W. Kalivas, S.A. Mackler, NAC-1, a rat brain mRNA, is increased in the nucleus accumbens three weeks after chronic cocaine self-administration, J. Neurosci. 17 (1997) 6864–6871.
[8] J. Wang, S. Rao, J. Chu, X. Shen, D.N. Levasseur, T.W. Theunissen, S.H. Orkin, A protein interaction network for pluripotency of embryonic stem cells, Nature 444 (2006) 364–368.
[9] J. Kim, J. Chu, X. Shen, J. Wang, S.H. Orkin, An extended transcriptional network for pluripotency of embryonic stem cells, Cell 132 (2008) 1049–1061.
[10] M. Malleshaiah, M. Padi, P. Rué, J. Quackenbush, A. Martinez-Arias, J. Gunawardena, Nac1 coordinates a sub-network of pluripotency factors to regulate embryonic stem cell differentiation, Cell Rep. 14 (2016) 1181–1194.
[11] K.L. Yap, P. Sysa-Shah, B. Bolon, R.C. Wu, M. Gao, A.L. Herlinger, F. Wang, F. Faiola, D. Huso, K. Gabrielson, T.L. Wang, J. Wang, M. Shih Ie, Loss of NAC1 expression is associated with defective bony patterning in the murine vertebral axis, PloS One 8 (2013) e69099.
[12] K. Nakayama, N. Nakayama, B. Davidson, J.J. Sheu, N. Jinawath, A. Santillan, R. Salani, R.E. Bristow, P.J. Morin, R.J. Kurman, T.L. Wang, M. Shih Ie, A BTB/POZ protein, NAC-1, is related to tumor recurrence and is essential for tumor growth and survival, Proc. Natl. Acad. Sci. U. S. A. 103 (2006) 18739–18744.
[13] K. Nakayama, N. Nakayama, T.L. Wang, M. Shih Ie, NAC-1 controls cell growth and survival by repressing transcription of Gadd45GIP1, a candidate tumor suppressor, Cancer Res. 67 (2007) 8058–8064.
[14] S. Yeasmin, K. Nakayama, M. Ishibashi, A. Katagiri, K. Iida, I.N. Purwana, N. Nakayama, K. Miyazaki, Expression of the bric-a-brac tramtrack broad complex protein NAC-1 in cervical carcinomas seems to correlate with poorer prognosis, Clin. Cancer Res. 14 (2008) 1686–1691.
[15] M. Ishibashi, K. Nakayama, S. Yeasmin, A. Katagiri, K. Iida, N. Nakayama, M. Fukumoto, K. Miyazaki, A BTB/POZ gene, NAC-1, a tumor recurrence-associated gene, as a potential target for Taxol resistance in ovarian cancer, Clin. Cancer Res. 14 (2008) 3149–3155.
[16] N. Jinawath, C. Vasoontara, K.L. Yap, M.M. Thiaville, K. Nakayama, T.L. Wang, I.M. Shih, NAC-1, a potential stem cell pluripotency factor, contributes to paclitaxel resistance in ovarian cancer through inactivating Gadd45 pathway, Oncogene 28 (2009) 1941–1948.
[17] M. Ishibashi, K. Nakayama, S. Yeasmin, A. Katagiri, K. Iida, N. Nakayama, K. Miyazaki, Expression of a BTB/POZ protein, NAC1, is essential for the proliferation of normal cyclic endometrial glandular cells and is up-regulated by estrogen, Clin. Cancer Res. 15 (2009) 804–811.
[18] M. Ishikawa, K. Nakayama, S. Yeasmin, A. Katagiri, K. Iida, N. Nakayama, K. Miyazaki, NAC1, a potential stem cell pluripotency factor expression in normal endometrium, endometrial hyperplasia and endometrial carcinoma, Int. J. Oncol. 36 (2010) 1097–1103.
[19] K. Nakayama, M.T. Rahman, M. Rahman, S. Yeasmin, M. Ishikawa, A. Katagiri, K. Iida, N. Nakayama, K. Miyazaki, Biological role and prognostic significance of NAC1 in ovarian cancer, Gynecol. Oncol. 119 (2010) 469–478.
[20] M. Shih Ie, K. Nakayama, G. Wu, N. Nakayama, J. Zhang, T.L. Wang, Amplification of the ch19p13.2 NACC1 locus in ovarian high-grade serous carcinoma, Mod. Pathol. 24 (2011) 638–645.
[21] S. Yeasmin, K. Nakayama, M.T. Rahman, M. Rahman, M. Ishikawa, A. Katagiri, K. Iida, N. Nakayama, Y. Otuski, H. Kobayashi, S. Nakayama, K. Miyazaki, Biological and clinical significance of NAC1 expression in cervical carcinomas: a comparative study between squamous cell carcinomas and adenocarcinomas/adenosquamous carcinomas, Hum. Pathol. 43 (2012) 506–519.
[22] T. Nishi, R. Maruyama, T. Urano, N. Nakayama, Y. Kawabata, S. Yano, M. Yoshida, K. Nakayama, K. Miyazaki, K. Takenaga, T. Tanaka, Y. Tajima, Low expression of nucleus accumbens-associated protein 1 predicts poor prognosis for patients with pancreatic ductal adenocarcinoma, Pathol. Int. 62 (2012) 802–810.
[23] K. Okazaki, N. Nakayama, Y. Nariai, H. Kato, K. Nakayama, K. Miyazaki, R. Maruyama, S. Kosugi, T. Urano, G. Sakashita, Nuclear localization signal in a cancer-related transcriptional regulator protein NAC1, Carcinogenesis 33 (2012) 1854–1862.
[24] P.H. Wu, S.H. Hung, T. Ren, M. Shih Ie, Y. Tseng, Cell cycle-dependent alteration in NAC1 nuclear body dynamics and morphology, Phys. Biol. 8 (2011) 015005.
[25] J. Ellenberg, E.D. Siggia, J.E. Moreira, C.L. Smith, J.F. Presley, H.J. Worman, J. Lippincott-Schwartz, Nuclear membrane dynamics and reassembly in living cells: targeting of an inner nuclear membrane protein in interphase and mitosis, J. Cell Biol. 138 (1997) 1193–1206.
[26] C.L. Wey, R.A. Cone, M.A. Edidin, Lateral diffusion of rhodopsin in photoreceptor cells measured by fluorescence photobleaching and recovery, Biophys. J. 33 (1981) 225–232.
[27] G. Carrero, D. McDonald, E. Crawford, G. de Vries, M.J. Hendzel, Using FRAP and mathematical modeling to determine the in vivo kinetics of nuclear proteins, Methods 29 (2003) 14–28.
[28] A.B. Houtsmuller, Fluorescence recovery after photobleaching: application to nuclear proteins, Adv. Biochem. Eng. Biotechnol. 95 (2005) 177–199.
[29] F. Mueller, D. Mazza, T.J. Stasevich, J.G. McNally, FRAP and kinetic modeling in the analysis of nuclear protein dynamics: what do we really know? Curr. Opin. Cell Biol. 22 (2010) 403–411.
[30] R.D. Phair, T. Misteli, High mobility of proteins in the mammalian cell nucleus, Nature 404 (2000) 604–609.
[31] N. Dross, C. Spriet, M. Zwerger, G. Muller, W. Waldeck, J. Langowski, Mapping eGFP oligomer mobility in living cell nuclei, PloS One 4 (2009) e5041.
[32] J. Lippincott-Schwartz, E. Snapp, A. Kenworthy, Studying protein dynamics in living cells, Nat. Rev. Mol. Cell Biol. 2 (2001) 444–456.
[33] A. Bancaud, S. Huet, G. Rabut, J. Ellenberg, Fluorescence perturbation techniques to study mobility and molecular dynamics of proteins in live cells: FRAP, photoactivation, photoconversion, and FLIP, Cold Spring Harb. Protoc. 2010 (2010) pdb top90.
[34] B. Davidson, A. Berner, C.G. Trope, T.L. Wang, M. Shih Ie, Expression and clinical role of the bric-a-brac tramtrack broad complex/poxvirus and zinc protein NAC-1 in ovarian carcinoma effusions, Hum. Pathol. 38 (2007) 1030–1036.
[35] L. Korutla, P.J. Wang, S.A. Mackler, The POZ/BTB protein NAC1 interacts with two different histone deacetylases in neuronal-like cultures, J. Neurochem. 94 (2005) 786–793.
[36] L. Korutla, R. Degnan, P. Wang, S.A. Mackler, NAC1, a cocaine-regulated POZ/BTB protein interacts with CoREST, J. Neurochem. 101 (2007) 611–618.
[37] N.J. Marianayagam, M. Sunde, J.M. Matthews, The power of two: protein dimerization in biology,, Trends Biochem. Sci. 29 (2004) 618–625.